

Fixed point behavior mapping of cumulants between the three-dimensional Ising model and QCD

Xue Pan^{1,*}

¹*School of Electronic Information and Electrical Engineering,
Chengdu University, Chengdu 610106, China*

Fixed point behavior was found in the temperature dependence of normalized cumulants of order parameter at different external magnetic fields in the three-dimensional Ising model in my last work. In this paper, considering possible existing QCD critical point belonging to the three-dimensional Ising universality class and the non-universal mapping parameters between the Ising model and QCD, effects of the mapping parameters on the fixed point behavior in the net-baryon chemical potential dependence of normalized cumulants along different experimental freeze-out curves is studied in this paper. We found that when the directions of Ising variables, the reduced temperature and external magnetic field, are orthogonal or not far from orthogonal after mapping to the QCD temperature and net-baryon chemical potential plane, the fixed point behavior exists in the net-baryon chemical potential dependence of the normalized cumulants and is closer to the QCD critical point than the peak in the cumulants.

PACS numbers: 25.75.Nq, 24.60.Ky

I. INTRODUCTION

One of the main goals of current relativistic heavy-ion collision experiments is to reveal the phase diagram of quantum chromo-dynamics (QCD) [1], where the location of the critical point, which is a unique character of the QCD phase diagram, is the most important. Recent years, high-order cumulants of multiplicity distributions of conserved charges, such as net-baryon, net-charge and net-strangeness, are suggested to search for the QCD critical point [2–5].

In the vicinity of the critical point, non-monotonic behavior of the high-order cumulants of conserved charges are found in a variety of QCD effective models and is regarded as critical related signal [5–8]. Particularly, when the critical point is approached on the crossover side, universal negative fourth-order cumulant of the order parameter is predicted in Ref. [9] and used to locate the QCD critical point in experiments [10]. While in Refs. [11, 12], the authors argued that the sign of high-order cumulants is not sufficient to prove the presence of the critical point. Other work indicate that the peak structure of kurtosis remains a solid feature and can be used as a clean signature of the critical point [13, 14]. Nevertheless the peak structure of cumulants can also occurs in a first order phase transition or crossover [15, 16]. Whether the non-monotonic or sign change behavior of high-order cumulants of conserved charges is reliable, accurate or enough to locate the critical point is uncertain.

In fact, the finite-size scaling, which implies a fixed point, can also be employed to locate the critical point [16–19]. Usually, the fixed point is obtained from the scale transformation of the re-normalization group,

resulting in the independence of rescaled thermodynamics on the system sizes at the critical point [20, 21].

In my recent work, the fixed point behavior has been found in the temperature dependence of normalized high-order cumulants of the order parameter at different fixed external magnetic fields in the three-dimensional Ising model [22]. What is more, the fixed point is just at the critical temperature of the Ising model.

The QCD critical point, if exists, is expected to belong to the same universality class of the three-dimensional Ising model [23–26]. Critical behavior of the corresponding thermodynamics in different systems that belongs to the same universality class is the same which is supervised by the same critical exponents. Recently, many works have been done to map the results of the three-dimensional Ising model to that of the QCD [14, 27].

In order to map the results of the Ising model to that of the QCD, usually, a linear ansatz between the QCD variables, temperature T and net-baryon chemical potential μ_B , and the Ising variables, reduced temperature t ($t = (\tau - \tau_c)/\tau_c$, where τ and τ_c are the temperature and critical temperature of the three-dimensional Ising model, respectively) and external magnetic field h is suggested [28–31]. Using three assumptions, firstly, the QCD system is in equilibrium, secondly, the linear map keep Ising t -direction and h -direction orthogonal to each other after mapped to the QCD $T - \mu_B$ phase diagram. At last, the freeze-out curves (FC) are below the crossover/first-order phase transition line, and parallel to the t -direction which has been mapped to the QCD phase diagram, the fixed point behavior has been found in the energy (transformation from the net-baryon chemical potential) dependence of normalized cumulants of order parameter in Ref. [22]. The fixed point is just at the critical energy (corresponding to the net-baryon chemical potential at the QCD critical point).

However, the mapping parameters are non-universal and far unknown from the Ising model to QCD. In this

*Electronic address: panxue1624@163.com

paper, on the assumption of the equilibrium of the QCD system, using parametric representation of the three-dimensional Ising model, we study and discuss the influences of the mapping parameters on the fixed point behavior in the net-baryon chemical potential dependence of normalized cumulants of order parameter along the experimental freeze-out curves. The freeze-out curves are also supposed below the crossover/first-order phase transition line, but are described by an empirical parametrization of the heavy-ion-collision data [32].

The paper is organized as follows. In section 2, the parametric representation and corresponding parametric expressions of second- to fourth-order cumulants of the three-dimensional Ising model is presented. The linear mapping from the three-dimensional Ising model to QCD is discussed. The experimental freeze-out curves are mapped to the Ising $t-h$ plane through different parameters. In section 3, net-baryon chemical potential dependence of the second- to fourth-order normalized cumulants is studied along the freeze-out curves. The effects of different mapping parameters on the net-baryon chemical potential dependence of the normalized cumulants are discussed. Finally, conclusions and summary are given in section 4.

II. THE LINEAR MAPPING FROM ISING TO QCD

In the parametric representation of the three-dimensional Ising model, magnetization M and reduced temperature t can be parameterized by two variables R and θ [33, 34],

$$M = m_0 R^\beta \theta, \quad t = R(1 - \theta^2). \quad (1)$$

The equation of state expressed by R and θ is

$$h = h_0 R^{\beta\delta} \tilde{h}(\theta). \quad (2)$$

Where m_0 in Eq. (1) and h_0 in Eq. (2) are normalization constants. They are fixed by imposing the normalization conditions $M(t = -1, h = +0) = 1$ and $M(t = 0, h = 1) = 1$. β and δ are critical exponents of the three-dimensional Ising universality class with values 0.3267(10) and 4.786(14), respectively [35].

One simple mean-field approximation of representation for $\tilde{h}(\theta)$ is as follows,

$$\tilde{h}(\theta) = \theta(3 - 2\theta^2). \quad (3)$$

When taking the approximate values of the critical exponents $\beta = 1/3$ and $\delta = 5$ (it is enough for our purpose), the first fourth order cumulants of magnetization (order parameter of the three dimensional Ising model) in the

parametric representation are as follows,

$$\begin{aligned} \kappa_1(R, \theta) &= m_0 R^{1/3} \theta, \\ \kappa_2(R, \theta) &= \frac{m_0}{h_0} \frac{1}{R^{4/3} (2\theta^2 + 3)}, \\ \kappa_3(R, \theta) &= \frac{m_0}{h_0^2} \frac{4\theta(\theta^2 + 9)}{R^3 (\theta^2 - 3)(2\theta^2 + 3)^3}, \\ \kappa_4(R, \theta) &= 12 \frac{m_0}{h_0^3} \frac{(2\theta^8 - 5\theta^6 + 105\theta^4 - 783\theta^2 + 81)}{R^{14/3} (\theta^2 - 3)^3 (2\theta^2 + 3)^5}. \end{aligned} \quad (4)$$

The reduced temperature t and external magnetic field h , are functions of R and θ provided by Eq. (1) and Eq. (2). Thus $\kappa_n(R, \theta)$ can be converted to $\kappa_n(t, h)$. At a negative h , the temperature dependence of second- to fourth-order cumulants all have a positive peak $\kappa_n^{max}(t, h)$ ($n = 2, 3, 4$). The cumulants can be normalized by their maximum at the peak as follows,

$$\kappa_n^{Norm}(t, h) = \kappa_n(t, h) / \kappa_n^{max}(t, h). \quad (5)$$

The fixed point behavior has been found in the temperature dependence of $\kappa_n^{Norm}(t, h)$ at different h in the three-dimensional Ising model. In order to map the results to that of the QCD, the following linear mapping relations are assumed,

$$\begin{aligned} \frac{T - T_c}{\Delta T} &= \sin \alpha_1 \frac{t}{\Delta t} + \sin \alpha_2 \frac{h}{\Delta h}, \\ \frac{\mu_B - \mu_{Bc}}{\Delta \mu_B} &= -\cos \alpha_1 \frac{t}{\Delta t} - \cos \alpha_2 \frac{h}{\Delta h}. \end{aligned} \quad (6)$$

Where T_c , μ_{Bc} are the temperature and net-baryon chemical potential at the QCD critical point. ΔT and $\Delta \mu_B$ denote the width of the critical regime in the QCD $T - \mu_B$ plane. Because the location of the critical point and the width of the critical regime for QCD are not known, the suggestion that $\Delta \mu_B \approx 0.1$ GeV from model calculations [36] and lattice QCD calculations [37] is used. We set $\Delta \mu_B = 0.1$ GeV and $\mu_{Bc} = 0.25$ GeV as was done in Ref. [38]. T_c is set as 0.165 GeV and $\Delta T/T_c = 1/8$.

Δt and Δh denote the width of the critical regime in the Ising $t-h$ plane. For details of defining the critical region, see Ref. [38]. After mapping t and h to the QCD $T - \mu_B$ phase diagram, α_1 is the angel between the t -direction and the opposite direction of μ_B axis, α_2 is the angel between the h -direction and the opposite direction of μ_B axis. A simply sketch of the mapping is shown in Fig. 1(a).

The freeze-out curve is assumed below the crossover/first-order phase transition line. An empirical parametrization of the heavy-ion-collision data from Ref. [32] can be used to describe the freeze-out curve,

$$T_f(\mu_B) = a - b\mu_B^2 - c\mu_B^4. \quad (7)$$

Where $a = 0.166$ GeV, $b = 0.139$ GeV⁻¹, $c = 0.053$ GeV⁻³.

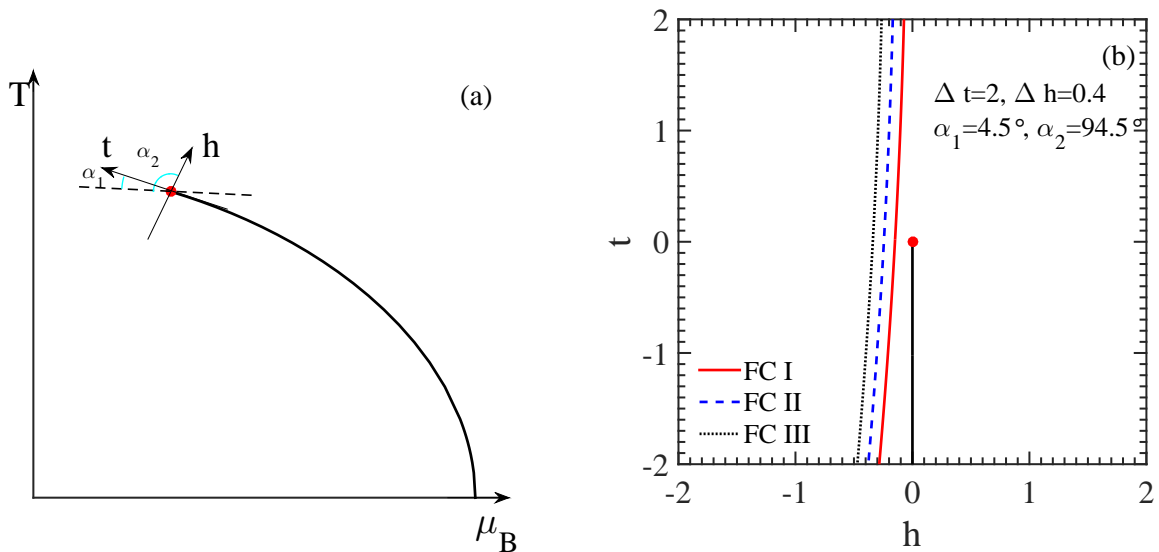


Abbildung 1: (Color online). A sketch of the mapping between QCD and Ising variables described by Eq. (6) (a), the mapping of three different freeze-out curves, FC I, FC II and FC III, given by Eqs. (7), (8) and (9) to the Ising $t-h$ plane by Eq. (6) for $\Delta t = 2$, $\Delta h = 0.4$, $\alpha_1 = 4.5^\circ$ and $\alpha_2 = 94.5^\circ$ (b), respectively.

According to the results in Refs. [39, 40], the chemical freeze-out temperature and net-baryon chemical potential could change as the centrality in the relativistic heavy-ion collisions. Although the temperature does not vary much, the net-baryon chemical potential increases from peripheral to central collisions [40]. For simplicity, we move the freeze-out curve described by Eq. (7) parallelly to the lower temperature side to get the other two freeze-out curves, i.e.,

$$T_{f1}(\mu_B) = a - b\mu_B^2 - c\mu_B^4 - 0.005, \quad (8)$$

and

$$T_{f2}(\mu_B) = a - b\mu_B^2 - c\mu_B^4 - 0.01. \quad (9)$$

Based on the mapping relation and using Eq. (6), these three freeze-out curves can be converted to three lines on the Ising $t-h$ plane. As an example, supposing $\Delta t = 2$, $\Delta h = 0.4$, the angles $\alpha_1 = 4.5^\circ$ and $\alpha_2 = 94.5^\circ$, a sketch of the mapping is shown in Fig. 1(b). The solid red, dashed blue and dotted black line from right to left represent the mapping of the freeze-out curves FC I, FC II and FC III presented by Eqs. (7), (8) and (9), respectively. It is clear that for each freeze-out curve after mapping to the Ising $t-h$ plane, the external magnetic field is not fixed as the cases in Ref. [22], but obvious fixed point behavior still can be observed in the temperature dependence of κ_2^{Norm} , κ_3^{Norm} and κ_4^{Norm} along these three freeze-out curves, which are presented in Fig. 2.

It is clear that the fixed point behavior exists in each sub-figure of Fig. 2. Although the temperature at the fixed point is not the critical temperature and a little bigger than the critical one, i.e. the fixed point is at the right side of the vertical green dashed line $t = 0$, it is still

in the vicinity of the critical temperature. What is more, the fixed point is closer to the vertical green dashed line than the peak in the cumulants.

III. FIXED POINT BEHAVIOR IN μ_B DEPENDENCE OF THE NORMALIZED CUMULANTS

Through the linear mapping relation between QCD and Ising variables represented by Eq. (6), t dependence of the cumulants in the Ising model can be converted to μ_B dependence. There are four parameters α_1 , α_2 , Δt and Δh . Along the t -direction, the symmetry is preserved. It is easy to realize that the t -direction should be tangential to the QCD first-order phase transition line at the critical point. As a result, the angle α_1 is usually not set very large [14]. Here it is fixed at 4.5° , which is close to the value in Ref. [14], where it is set as 4.6° . For the h -direction after mapping to QCD, there is no general rule. To set the h -direction orthogonal to the t -direction is the common and simply choice in the literature. That is $\alpha_2 = 94.5^\circ$ here. To study the influence of h -direction slightly deviated from the orthogonal direction of t , the other two values are also chosen for α_2 . They are 72° and 117° , respectively. What is more, α_2 and $\alpha_2 \pm \pi$ are equivalent for the mapping since the sign of h is a matter of convention.

After the values of Δt and Δh are set as 2 and 0.4, respectively, the influence of α_2 on the fixed point behavior in the μ_B dependence of the normalized second- to fourth-order cumulants are studied and shown in Fig. 3.

In each sub-figure of Fig. 3, the vertical dashed green line $\mu_B = \mu_{Bc}$ shows the critical net-baryon chemical po-

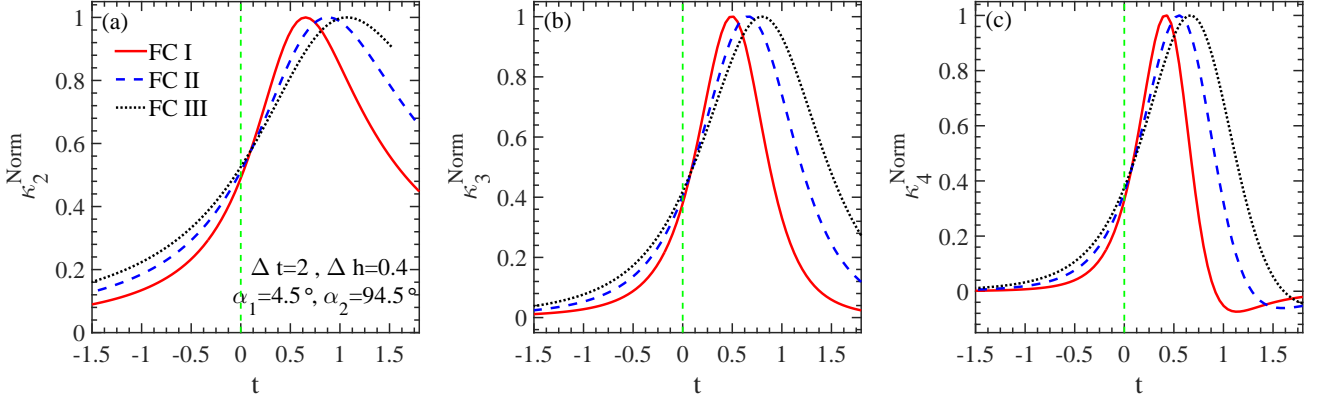


Abbildung 2: (Color online). Temperature dependence of κ_2^{Norm} , κ_3^{Norm} , and κ_4^{Norm} for $\Delta t = 2$, $\Delta h = 0.4$, $\alpha_1 = 4.5^\circ$ and $\alpha_2 = 94.5^\circ$ along the three different freeze-out curves, respectively. The vertical green dashed line shows the critical temperature $t = 0$.

tential. The solid red curve, dashed blue curve and dotted black curve represent the μ_B dependence of the normalized cumulants along the three freeze-out curves represented by Eq. (7), Eq. (8) and Eq. (9), respectively. The qualitative μ_B dependence of each order cumulant does not change along the different freeze-out curves. They all have a peak when approaching μ_{Bc} from the smaller μ_B side. The peak gets sharper and closer to the vertical dashed green line when the freeze-out curve gets closer to the phase boundary. I.e. the peak is sharpest in the solid red curve and it is closest to the vertical dashed green line. And the case is just opposite in the dotted black curve.

It is clear that the μ_B dependence of normalized cumulants along three different freeze-out curves intersect at a point. Except for κ_4^{Norm} at $\alpha_2 = 72^\circ$ in Fig. 3(c), the fixed points are all at the right side of the peaks and closer to the vertical dashed green line than the peaks.

With the three different values of α_2 chosen here, the fixed point behavior all exits, while the position of the fixed point moves a little. In the top row of Fig. 3, $\alpha_2 = 72^\circ$, the fixed point is at the left side of the vertical dashed green line. μ_B of the fixed point is smaller than μ_{Bc} . With $\alpha_2 = 94.5^\circ$, i.e. the middle row of Fig. 3, the fixed point is nearly on the vertical dashed green line. Its μ_B is very close to μ_{Bc} . While with $\alpha_2 = 117^\circ$, i.e. the bottom row of Fig. 3, the fixed point is at the right side of the vertical dashed green line. Its μ_B is a little larger than μ_{Bc} . What is more, as the increase of α_2 , the value of κ_2^{Norm} , κ_3^{Norm} and κ_4^{Norm} at the fixed point all decreases. And the higher the order of the normalized cumulants, the faster its value changes with α_2 .

Although it is not shown here, it should be clarified that if α_2 continues to decrease, the fixed point will come to the left side of the peak, just like the case in Fig. 3(c), then the peak will be closer to μ_{Bc} . In reverse, if α_2 continues to increase, the value of the normalized cumulant at the fixed point along the three freeze-out curves will approach to zero, just like the case in Fig.3 (i). If α_2

approaches to α_1 or $\pi \pm \alpha_1$, that is the t -direction and h -direction are nearly parallel to each other after mapped to the QCD $T - \mu_B$ plane, the three freeze-out curves will not pass through or even reach the critical region of the Ising model. The fixed point behavior in the t dependence of the normalized cumulants along the freeze-out curves does not exist any more.

On the whole, when the h -direction and t -direction after mapping to the QCD phase diagram is orthogonal or not far from orthogonal, the fixed point behavior exists in μ_B dependence of normalized cumulants along different freeze-out curves and is closer to μ_{Bc} than the peak in the cumulants. While the value of α_2 will influence the position of the fixed point. When h -direction and t -direction are nearly orthogonal to each other, μ_B of the fixed point is closer to μ_{Bc} .

To discuss the effects of Δt and Δh on the fixed point behavior in μ_B dependence of the normalized cumulants, Δt is taken three different values 1, 2 and 4. Δh is also taken three different values 0.1, 0.2 and 0.4. While the angles α_1 and α_2 are fixed at 4.5° and 94.5° , respectively. The influence of the change of Δt and Δh on the fixed point behavior in κ_2^{Norm} , κ_3^{Norm} and κ_4^{Norm} are the same. For simplicity, let us take κ_2^{Norm} as an example. The net-baryon chemical potential dependence of κ_2^{Norm} is shown in Fig. 4. Results along the three freeze-out curves are still represented by the solid red curve, dashed blue curve and dotted black curve, respectively. The vertical dashed green line shows the critical net-baryon chemical potential.

In each column, the value of Δh is fixed and the value of Δt increases from top to bottom. It is clear that as Δt gets bigger, the peak in κ_2^{Norm} gets sharper. The position of fixed point shift to the bigger μ_B side a little. At the same time, the value of κ_2^{Norm} at fixed point gets a little smaller. In each row, the value of Δt is fixed while the value of Δh increases from left to right. It is clear that the peak in κ_2^{Norm} gets flatter as Δh gets bigger. The position of fixed point shift to the smaller μ_B side a little.

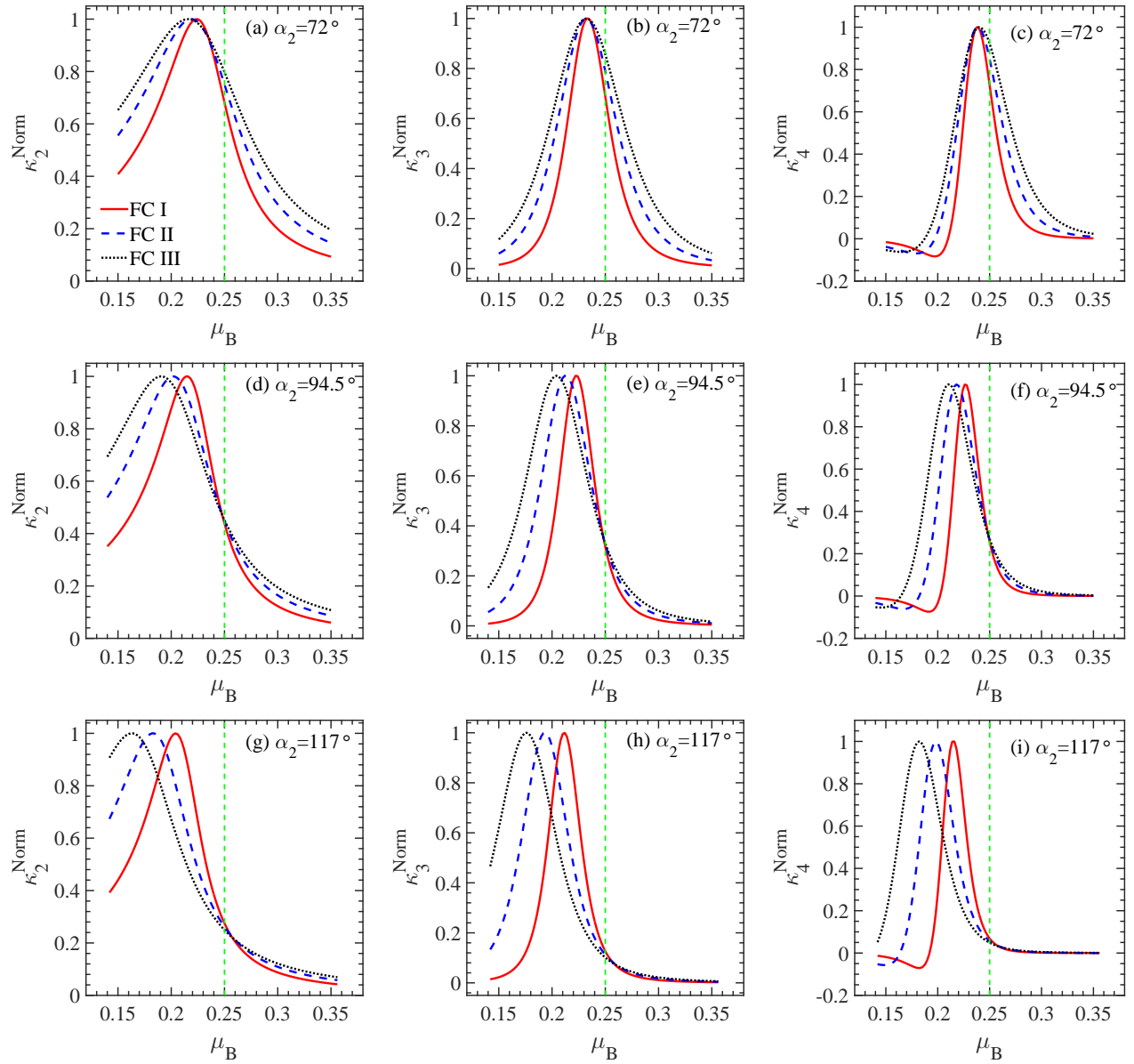


Abbildung 3: (Color online). Net-baryon chemical potential dependence of κ_2^{Norm} , κ_3^{Norm} , and κ_4^{Norm} at $\alpha_2 = 72^\circ$ (up panels), 94.5° (middle panels) and 117° (down panels) with $\alpha_1 = 4.5^\circ$, $\Delta t = 2$ and $\Delta h = 0.4$ along three different freeze-out curves, respectively. The green dashed line shows the net-baryon chemical potential at the QCD critical point.

Meanwhile the value of κ_2^{Norm} at fixed point gets a little bigger.

So the trend of the influence of Δt and Δh on the normalized cumulants and position of fixed point is just opposite. Smaller Δt and bigger Δh lead to flatter peak in μ_B dependence of κ_2^{Norm} and the move of the fixed point to the smaller μ_B side, i.e. the peak of κ_2^{Norm} in Fig. 4(c) is the flattest and the value of μ_B at the fixed point is the smallest. One more thing to note is that the position of the fixed point is all close to the vertical dashed green line in each sub-figure.

On the whole, the influence of Δt and Δh on the fixed point behavior is not so great as that of α_2 . In all case, the

fixed point exists and is close to the critical net-baryon chemical potential when the t -direction and h -direction are nearly orthogonal.

Turning to the heavy-ion collision experiments, the energy (\sqrt{s}) dependence of the normalized cumulants can be got from the relation between μ_B and \sqrt{s} given in Ref. [32], for details to see Ref. [22]. It is easy to realize that the fixed point behavior also exists in the energy dependence of the normalized cumulants along the three different freeze-out curves as long as the t -direction and h -direction is not far from orthogonal to each other after mapped to the QCD $T - \mu_B$ plane. Based on the universality of the critical behavior, the fixed point be-

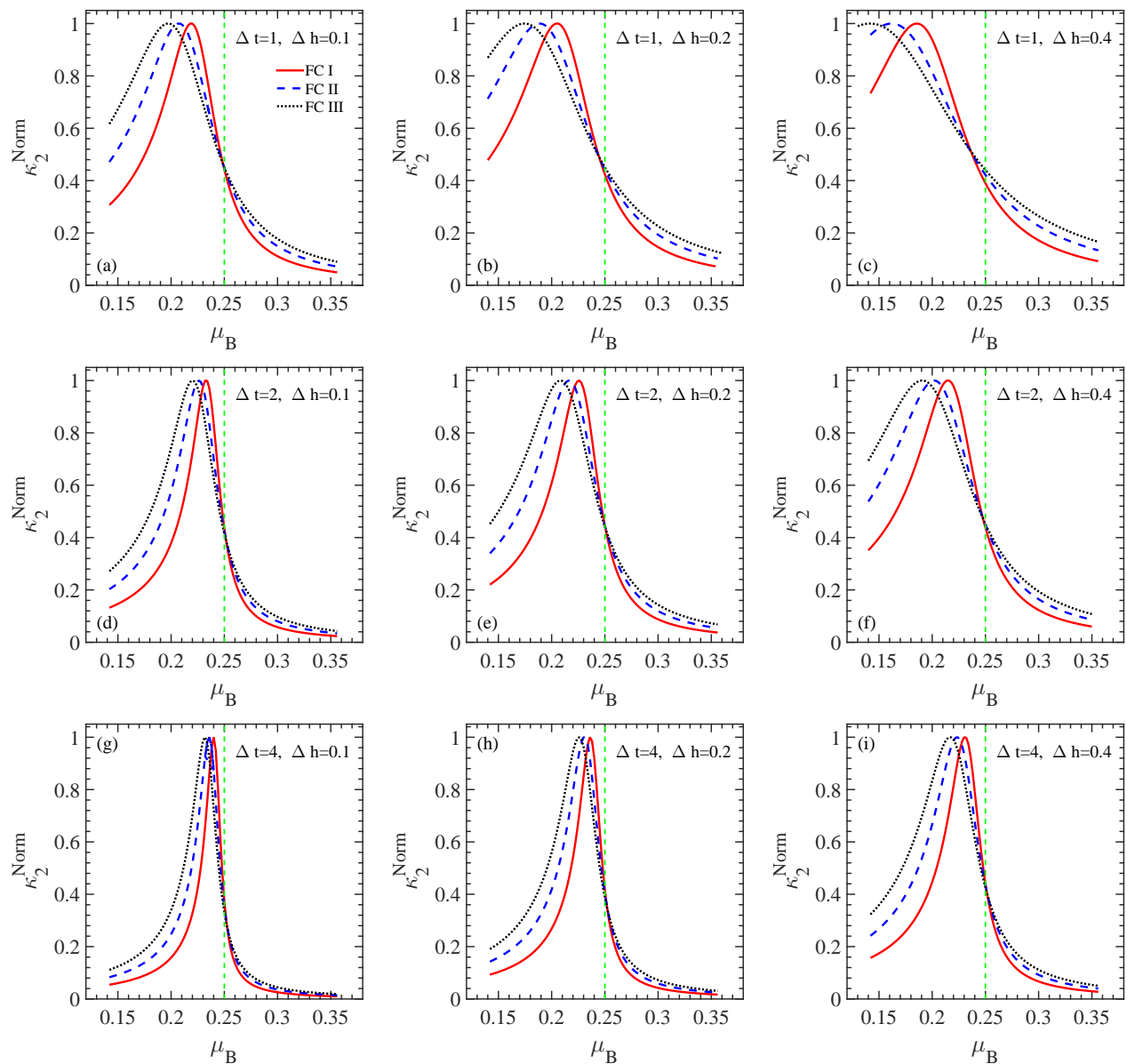


Abbildung 4: (Color online). Net-baryon chemical potential dependence of κ_2^{Norm} at different Δt and Δh along three different freeze-out curves. $\Delta t = 1, 2$ and 4 for the up, middle and down panels, respectively. $\Delta h = 0.1, 0.2$ and 0.4 for the left, middle and right panels, respectively. The green dashed line shows the net-baryon chemical potential at the QCD critical point.

havior may be used to locate the QCD critical point in the relativistic heavy-ion collision experiments.

IV. SUMMARY

Through a linear mapping relation from the three-dimensional Ising model to QCD, the experimental freeze-out curves are mapped to the Ising $t-h$ plane. By using the parametric representation of the three-dimensional Ising model and the linear mapping relation, the net-baryon chemical potential dependence of normalized second- to fourth-order cumulants of the order para-

meter along three different freeze-out curves are studied.

Fixed point behavior is observed in the net-baryon chemical potential dependence of the normalized cumulants along three different freeze-out curves when the h -direction and t -direction is orthogonal or not far from orthogonal after mapping to the QCD $T-\mu_B$ phase plane. The fixed point is closer to the net-baryon chemical potential of QCD critical point than the peak of the cumulants.

The influence of three mapping parameters α_2 , Δt and Δh , on the net-baryon chemical potential dependence of the normalized cumulants and the fixed point behavior is discussed. As the increase of α_2 , that is from 72°

to 117° here, the net-baryon chemical potential at the fixed point increases, while the corresponding value of normalized cumulants decreases. When the t -direction and h -direction are nearly orthogonal to each other, the net-baryon chemical potential at the fixed point is much closer to the one at the QCD critical point.

The two parameters describing the width of the critical region of the three-dimensional Ising model, Δt and Δh , have great influence on the behavior of cumulants, but little influence on the fixed point behavior. As the increase of Δt and decrease of Δh , the peak in the net-baryon chemical potential dependence of the cumulants

gets sharper, while the net-baryon chemical potential at the fixed point get a little bigger but not so obvious. And the values of μ_B at the fixed point are all close to that of μ_{Bc} when the t -direction and h -direction are orthogonal.

Fixed point behavior also exists in the energy dependence of the normalized cumulants along the experimental freeze-out curves when the t -direction and h -direction is orthogonal or not far from orthogonal after mapping to the QCD $T - \mu_B$ plane. It may be used to locate the QCD critical point in the relativistic heavy-ion collision experiments.

-
- [1] J. Adams et al (STAR Collaboration), *Nucl. Phys. A* **757** (2005) 102.
- [2] B. Friman, F. Karsch, K. Redlich et al, *Eur. Phys. J. C* **71** (2001) 1694.
- [3] Y. Hatta, M. A. Stephanov, *Phys. Rev. Lett.* **91** (2003) 102003.
- [4] V. Koch, arXiv:0810.2520.
- [5] M. A. Stephanov, *Phys. Rev. Lett.* **102** (2009) 032301.
- [6] M. Asakawa, S. Ejiri, M. Kitazawa, *Phys. Rev. Lett.* **103** (2009) 262301.
- [7] V. Skokov, B. Friman and K. Redlich, *Phys. Rev. C* **83** (2011) 054904.
- [8] Wei-jie Fu, Yu-Xin Liu, and Yue-Liang Wu, *Phys. Rev. D* **81** (2010) 014028.
- [9] M. A. Stephanov, *Phys. Rev. Lett.* **107** (2011) 052301.
- [10] S. Collaboration, L. Adamczyk, J. K. Adkins, et al., *Phys. Rev. Lett.* **112** (2014) 032302.
- [11] W. Fan, X. Luo and H. Zong, *Chin. Phys. C* **43** (2019) 033103.
- [12] Li-Zhu Chen, Ye-yin Zhao, Jin Wu, et al., *Chin. Phys. C* **45** (2021) 104103.
- [13] Z. Li, K. Xu, X. Wang and M. Huang, *Eur. Phys. J. C* **79** (2019) 245.
- [14] D. Mroczek, A. R. Nava Acuna, J. Noronha-Hostler et al., *Phys. Rev. C* **103** (2021) 034901.
- [15] Y. Aoki, G. Endrödi, Z. Fodor et al, *Nature* **443** (2006) 675.
- [16] Xue Pan, Mingmei Xu and Yuanfang Wu, *J. Phys. G: Nucl. Part. Phys.* **42** (2015) 015104.
- [17] N. G. Antoniou, F. K. Diakonou, X. N. Maintas and C. E. Tsagkarakis, *Phys. Rev. D* **97** (2018) 034015.
- [18] Y. Zhang, Y. Zhao, L. Chen, X. Pan, M. Xu, Z. Li, Y. Zhou and Y. Wu, *Phys. Rev. E* **100** (2019) 052146.
- [19] L. Chen, Y. Zhao, X. Li, Z. Li and Y. Wu, *Int. Jour. Mod. Phys. E* **30** (2021) 2150056.
- [20] M. E. Fisher, *Rev. Mod. Phys.* **46** (1974) 597.
- [21] K. Wilson, *Phys. Rep.* **12** (1974) 75.
- [22] Xue Pan, *Chin. Phys. C* **46** (2022) 024104.
- [23] P. de Forcrand, O. Philipsen, *Phys. Rev. Lett.* **105** (2010) 152001.
- [24] M. Stephanov, K. Rajagopal, E. Shuryak, *Phys. Rev. Lett.* **81** (1998) 4816.
- [25] M. Asakawa, *J. Phys. G: Nucl. Part. Phys* **36** (2009) 064042.
- [26] R. D. Pisarski, F. Wilczek, *Phys. Rev. D* **29** (1984) 338.
- [27] M. Caselle and M. Sorba, *Phys. Rev. D* **102** (2020) 014505.
- [28] J.J. Rehr and N.D. Mermin, *Phys. Rev. A* **8** (1973) 472.
- [29] N. B Wilding, *J. Phys.: Condens. Matter* **9** (1997) 585.
- [30] C. Nonaka and M. Asakawa, *Phys. Rev. C* **71** (2005) 044904.
- [31] Xue pan, Lizhu Chen, X.S. Chen and Yuanfang Wu, *Nucl. Phys. A* **913** (2013) 206.
- [32] J. Cleymans, H. Oeschler, K. Redlich and S. Wheaton, *Phys. Rev. C* **73** (2006) 034905.
- [33] P. Schofield, *Phys. Rev. Lett.* **22** (1969) 606.
- [34] D. J. Wallace, R. K. P. Zia, *J. Phys. C: Solid State Phys* **7** (1974) 3480.
- [35] H. W. J. Blöte, E. Luijten, J. R. Heringa, *J. Phys. A: Math. Gen* **28** (1995) 6289.
- [36] Y. Hatta and T. Ikeda, *Phys. Rev. D* **67** (2003) 014028.
- [37] R. V. Gavai and S. Gupta, *Phys. Rev. D* **78** (2008) 114503.
- [38] S. Mukherjee, R. Venugopalan and Y. Yin, *Phys. Rev. C* **92** (2015) 034912.
- [39] J. Cleymans, B. Kämpfer, M. Kaneta, S. Wheaton and N. Xu, *Phys. Rev. C* **71** (2005) 054901.
- [40] D. Biswas, *Advances in High Energy Physics* **2021** (2021) 6611394.